aggregate near the boojum, the defect becomes a bridge between two defect shells that join both particles, depicted in insert (c); coincidentally, the bridge is more notorious in configurations with larger free energy.

Configurations with the maximum free energy correspond with particles scattered throughout the droplet surface in a greater degree than states with lower energy. For all set sizes we found degenerate states, characterized by more traveling particles.

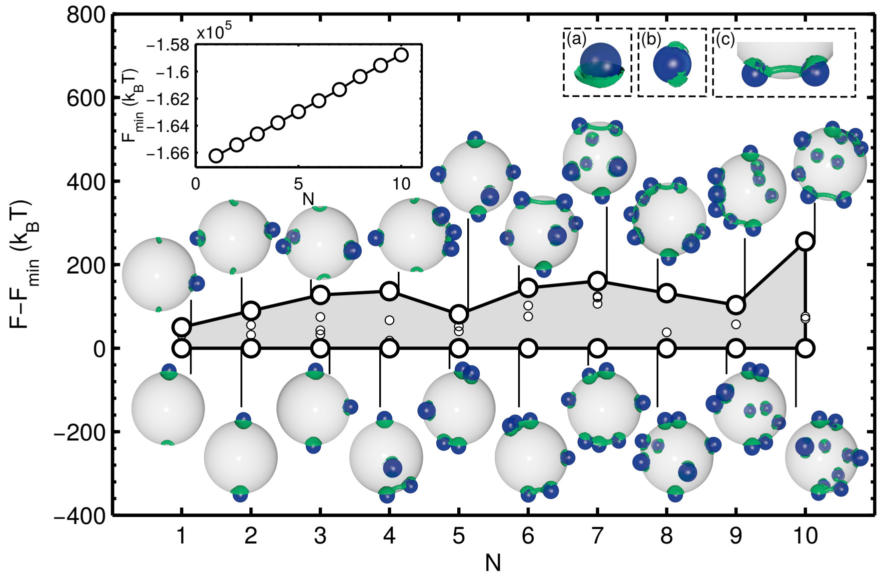

Figure 5.4. Free energy difference for planar particles with anchoring strength $W = 1 \times 10^{-3}$ J/m^2, with the minimum free energy for each N as the reference shown in the insert. Small round markers indicate metastable configurations (not shown), while big markers represent configurations with the maximum and minimum free energy density. The inserts show the defect structure exhibited by nanoparticles positioned on (a) the boojum of the bipolar droplet, and (b) the equator. (c) Bridge defect between two nanoparticles near the boojum location.

Moderate anchoring conditions, $W = 1 \times 10^{-4}$ J/m^2, broaden the spectrum of possible arrays as evidenced in figure 5.5. Only for $N = 2$ and $N = 3$ there is no degeneracy and the particles arrange in opposite poles. Defects surround the submerged hemisphere of nanoparticles and some common arrangements are found when particles aggregate near the boojum region. Similar to the homeotropic case, assembly in linear, triangular, and diamond shaped patterns are observed as depicted in inserts (a)-(e) in figure 5.5. In resemblance to cases with stronger anchoring, states with higher free energy correspond to particles being scattered on the surface in an unbiased